Diabetes-specific regulation of adipocyte metabolism by the adipose tissue extracellular matrix

Nicki A. Baker, Lindsey A. Muir, Alexandra R. Washabaugh, Christopher K. Neeley, Sophie Yu-Pu Chen, Carmen G. Flesher, John Vorwald, Jonathan F. Finks, Amir A. Ghaferi, Michael W. Mulholland, Oliver A. Varban, Carey N. Lumeng, Robert W. O'Rourke

The Journal of Clinical Endocrinology & Metabolism
Endocrine Society

Submitted: August 07, 2016
Accepted: December 30, 2016
First Online: January 05, 2017

The Journal of Clinical Endocrinology & Metabolism; Copyright 2017 DOI: 10.1210/jc.2016-2915

Diabetes-specific regulation of adipocyte metabolism by the adipose tissue extracellular matrix

Nicki A. Baker[1], Lindsey A. Muir[2], Alexandra R. Washabaugh[1], Christopher K. Neeley[1], Sophie Yu-Pu Chen[5], Carmen G. Flesher[6], John Vorwald[6], Jonathan F. Finks[1], Amir A. Ghaferi[1,7], Michael W. Mulholland[1], Oliver A. Varban[1], Carey N. Lumeng[2,3,4], Robert W. O'Rourke[1,7]

[1]Department of Surgery, [2]Department of Pediatrics and Communicable Diseases, [3]Graduate Program in Immunology, and [4]Graduate Program in Cellular and Molecular Biology, University of Michigan Medical School, Ann Arbor, MI, USA; [5]Center for Statistical Consultation & Research, and [6]Undergraduate Research Opportunity Program, University of Michigan, Ann Arbor, MI, USA; [7]Department of Surgery, Ann Arbor Veteran's Administration Hospital, Ann Arbor, MI, USA

Received 07 August 2016. Accepted 30 December 2016.

Abbreviations: body mass index (BMI), counts per minute (cpm), diabetes/diabetic (DM); extracellular matrix (ECM); fetal calf serum (FCS); hemoglobin A1c (HbA1c); hexamethyldisalizane (HMDS), non-diabetic (NDM), phenylmethanesulphonylfluoride (PMSF), quantitative real-time polymerase chain reaction (QRTPCR), subcutaneous adipose tissue (SAT), scanning electron microscopy (SEM), visceral adipose tissue (VAT)

Context: The role of the extracellular matrix (ECM) in regulating adipocyte metabolism in the context of metabolic disease is poorly defined.
Objective: To define the metabolic phenotype of adipocytes associated with human diabetes and the role of the ECM in regulating adipocyte metabolism
Design: Adipose tissues from obese patients were studied in standard 2D-culture and an *in vitro* model of decellularized adipose tissue ECM repopulated with human adipocytes, and results correlated with diabetes status.
Setting: Academic University Medical Center and Veteran's Administration Hospital
Patients: 70 patients with morbid obesity undergoing bariatric surgery
Interventions: Visceral and subcutaneous adipose tissues collected at the time of bariatric surgery
Outcome measures: Metabolic assays for glucose uptake, lipolysis, and lipogenesis in adipocytes in 2D-culture and 3D-ECM culture
Results: Adipocytes from diabetic subjects manifest decreased glucose uptake and decreased lipolysis in 2D-culture. ECM supports differentiation of mature adipocytes and recapitulates diabetes-specific differences in adipocyte metabolism observed in 2D-culture. ECM from non-diabetic subjects partially rescues glucose uptake and lipolytic defects in adipocytes from diabetic subjects, while ECM from diabetic subjects impairs glucose uptake in adipocytes from non-diabetic subjects.
Conclusions: Diabetes is associated with adipocyte metabolic dysfunction. The ECM regulates adipocyte metabolism. Non-diabetic ECM rescues metabolic dysfunction in diabetic adipocytes, while diabetic ECM imparts features of metabolic dysfunction to non-diabetic adipocytes. These findings suggest the ECM as a target for manipulating adipose tissue metabolism.

Precis: An *in vitro* model of adipose tissue extracellular matrix repopulated with adipocytes was used to demonstrate that the extracellular matrix regulates adipocyte metabolism in a disease-specific manner.

INTRODUCTION:

Adipose tissue metabolic dysfunction contributes to systemic metabolic disease, including type II diabetes (DM), but precise cellular metabolic alterations and underlying mechanisms remain poorly defined. Quantitative and qualitative changes in the adipose tissue extracellular matrix (ECM) have been associated with metabolic disease and may contribute to adipocyte dysfunction (1-6). Nonetheless, the relationship between adipose tissue fibrosis and human diabetes is unclear, and robust *in vitro* models of adipocyte-ECM interactions are lacking. The goals of this study were to address these knowledge gaps and examine the hypothesis that the ECM regulates adipocyte metabolism in a disease-specific manner.

METHODS:

Human subjects:

Human subjects undergoing bariatric surgery were enrolled with Institutional Review Board approval at the University of Michigan and Ann Arbor Veteran's Administration Hospitals. Visceral adipose tissue (VAT) from the greater omentum and subcutaneous adipose tissue (SAT) from the abdominal wall was collected from 70 subjects. Diabetic (DM) subjects were defined by clinical diagnosis of type 2 diabetes requiring treatment with medication and hemoglobinA1c (HbA1c)>=6.5%. Non-diabetic (NDM) subjects were defined by no clinical history of diabetes and hemoglobinA1c (HbA1c) <6.5% per American Diabetes Association criteria (7).

Preadipocyte isolation, adipocyte 2D-culture:

Adipose tissue was digested with Type II collagenase (2mg/mL in PBS/2% BSA, Life Technologies Inc., Carlsbad, CA, USA) 37^{o}C, 60min, centrifuged 250rcf, and the stromal-vascular cell pellet retrieved, plated overnight, and adherent cells passaged 3X to enrich for preadipocytes, which were frozen in DMEM/F12, 15% fetal calf serum (FCS), 10% DMSO in liquid nitrogen. To generate mature adipocytes, preadipocytes (60,000 cells/well in 24-well plates) were plated in DMEM/F12, 15% FCS until confluent, cultured 7days in differentiation medium (DMEM/F12, 2.5mM glutamine, 15mM HEPES, 10mg/ml transferrin, 33µM biotin, 0.5µM human insulin, 17µM pantothenate, 0.1µM dexamethasone, 2nM T3, 540µM IBMX, 1µM ciglitazone), then cultured 7days in maintenance medium (DMEM/F12, 2.5mM glutamine, 15mM HEPES, 10mg/ml transferrin, 33µM biotin, 0.5µM human insulin) until differentiated.

ECM preparation:

ECM isolation was modified from published protocols for adipose and lung tissues (8-10). VAT explants (1gm) were freeze-thawed in 10mM Tris, 5mM EDTA, 1% phenylmethanesulphonylfluoride (PMSF), pH8.0 from -80^{0}C, 20 min to 37^{0}C, 5min 3X, incubated 37^{0}C, 24hrs in 0.25% Trypsin/0.1%EDTA; washed in rinsing buffer (8g/L NaCl, 200mg/L KCl, 1g/L Na_2HPO_4, 200mg/L KH_2PO_4, 1% PMSF), 37^{0}C, 20min 3X; incubated 37^{0}C, 24hrs in 55mM Na2HPO4, 17mM KH_2PO_4, 4.9mM $MgSO_4$*7H_2O, 160U/mL DNase I type II, 100µg/mL RNase type IIIA, 80U/mL lipase type VI-S (Sigma-Aldrich Inc., St. Louis MO, USA), 1% PMSF; washed sequentially in rinsing buffer 37^{0}C, 20min 3X; 99.9% isopropanol, 1% PMSF 25^{0}C 1X, 24hrs; rinsing buffer 37^{0}C, 20min 3X; 70% EtOH, 37^{0}C, 20min 3X; and storage solution (PBS, 1% PMSF) 37^{0}C, 20min 1X; then stored in storage solution 4^{0}C.

ECM-adipocyte culture:

Decellularized ECM tissue was rinsed in 70% EtOH, rehydrated in PBS, cut/weighed into 100mg fragments, seeded with 60,000 preadipocytes in 20µL of complete growth medium (DMEM, 10% FCS), incubated 37^{o}C, 5%CO_2, 40min to allow cells to adhere, then 0.5mL of complete growth medium added, incubated 37^{o}C, 5%CO_2, 24hrs, transferred to a fresh culture

plate, 0.5mL of complete growth medium added, cultured 3days, then cultured in 0.5mL differentiation medium 14days to generate mature adipocytes in ECM.

Collagen I immunohistohemistry:
Adipose tissue or ECM were fixed in 10% formalin, paraffin-embedded, sectioned onto slides, heat-treated, deparaffinized, rehydrated, heat-induced epitope retrieval performed with FLEX-TRS High pH Retrieval buffer (Dako-Agilent Technologies Inc. Glostrup, Denmark), stained with rabbit polyclonal collagen I-alpha-1 antibody (Thermo Scientific, Inc., Kalamazoo, MI, USA, 1:1000), and FLEX-HRP-EnVision System used for detection (Dako-Agilent Technologies Inc.). Slides were counterstained with hematoxylin and imaged on an Olympus IX 81 microscope.

Oil Red-O staining:
Adipose tissue or ECM-adipocytes frozen in liquid nitrogen and cut into 5µm sections onto slides were stained with Oil Red-O Stain Kit (American Master Tech Scientific Inc., Lodi, CA, USA) and imaged on an Olympus IX-81 microscope. Adipocytes in 2D culture were washed with 1X PBS, fixed in 4% formalin then 60% isopropanol, stained with 200µL Oil Red-O Stain Kit, washed in PBS, air-dried, resuspended in 200µL 100% isopropanol and absorbance read at 525nM on an Epoch Microplate spectrophotometer (BioTek Instruments, Inc., Winooski, VT, USA).

Scanning electron microscopy:
Tissues were fixed in Sorensen's phosphate buffer, 2.5% glutaraldehyde, 25^0C, 12hrs; post-fixed in Sorensen's buffer, 1% osmium tetroxide, 4^0C, 1hr; serially dehydrated in EtOH, washed in hexamethyldisalizane (HMDS), air-dried, mounted on SEM-stub with colloidal graphite, dried, sputter-coated with gold, and images captured on an Amray 1910 scanning electron microscope (Amray Inc., Bedford, MA, USA) using SEMTech Solutions X-Stream Image-Capture software (SEMTech Solutions Inc., Billerica, MA, USA).

Glucose uptake:
Adipocytes in 2D-culture or 3D-ECM were cultured 37°C, 72hrs in 0.5mL maintenance medium; then in serum-free DMEM:F12, 37°C, 12hrs; in PBS/1% BSA, 37°C, 2hrs; washed in PBS, then cultured in 0.5mL PBS+/-100nM human insulin, 37°C, 40min; in 0.5mL PBS+/-200nM insulin, 0.1mM 2-deoxy glucose (Sigma-Aldrich Inc.), 2µCi/mL deoxy-D-glucose-2-[1,2-^{3}H(N)] (PerkinElmer Inc., Waltham, MA, USA) 37°C, 40min, then washed with PBS, and 420µL 1% SDS solution added, and cells lysed with pipetting. 10µL of cell lysate was used for Bradford protein assay; 400µL of lysate was transferred to 2mL scintillation fluid and counts per minute (cpm) measured on a scintillation counter and normalized to cell lysate protein concentration.

Lipogenesis:
Lipogenesis assay was modified from published protocols (11, 12). Adipocytes in 2D-culture or 3D-ECM were cultured 37°C, 72hrs in 0.5mL maintenance medium; washed with PBS; cultured 37°C, 24hrs in 0.5mL serum starvation medium (DMEM:F12, 100nM insulin); cultured 37°C, 24hrs in 0.5mL lipogenesis medium (serum starvation medium + 10µM sodium acetate, 0.5µCi 3H-acetate (PerkinElmer Inc., Waltham, MA, USA)), washed with PBS, then 120µL 0.1N HCl added, followed by pipetting to lyse cells. 10µL of lysate was used for Bradford protein assay; 100µL of lysate was added to 500µL of 2:1 chloroform:methanol (v/v), incubated 25^0C, 5min; 250µL H_2O added, incubated 25^0C, 5min, centrifuged 3,000rcf, 25^0C, 10min, and lipid phase transferred to 2mL scintillation fluid, and cpm measured on a scintillation counter and

normalized to cell lysate protein concentration. For "no insulin" arm, cells were cultured in serum starvation medium lacking insulin; for "insulin+C75" arm, cells were cultured in serum starvation medium with insulin and C75, 10µg/ml.

Lipolysis:
Adipocytes in 2D- or 3D-ECM culture were cultured 37^{o}C, 72hrs in 0.5mL maintenance medium +/- 3µM isoproterenol, then glycerol concentration in supernatants measured with a lipid metabolite assay kit (Sigma-Aldrich, Inc.) and normalized to either cell lysate protein concentration measured by Bradford assay or cell lysate DNA concentration measured by CyQuant assay (Thermo Scientific, Inc., Kalamazoo, MI, USA).

QRTPCR:
Adipocytes in 2D-culture were lysed in Trizol, and ECM-adipocyte cultures were homogenized with a BeadBug Homogenizer (Benchmark Scientific Inc., Edison, NJ, USA), and RNA extracted with RNAEasy Fibrous Tissue MiniKit (Qiagen Inc., Hilden, Germany). Equal amounts of input RNA were reverse-transcribed and quantitative real-time polymerase chain reaction (QRTPCR) performed using Taqman primer-probes (Life Technologies Inc., Carlsbad, CA, USA) with actin as an endogenous control on a StepOnePlus thermocycler (Applied Biosystems Inc., Foster City, CA, USA). The 2^{-dCT} method was used to calculate fold differences in transcript levels, setting undetermined values at dCT=40.

Statistical analysis:
Paired or independent t-test was used to compare continuous data between groups. Fisher's exact test was used to compare dichotomous demographic variables. Delta CT values were compared for QRTPCR data from 2D culture, adjusting for age and gender. Linear regression was used to determine correlations. Analysis of covariance using general linear models was used to compare outcome measures while adjusting for age and gender as covariates. For ECM-AD experiments, to account for possible correlation within subjects given that data involve repeated measures, a linear mixed model with random intercepts for subject matrix and subject cell was used to compare metabolic and QRTPCR (dCT values) data between arms while simultaneously adjusting for age and gender of subjects from whom both ECM and preadipocytes were derived. Correlations of HbA1c-ECM or HbA1c-AD as continuous variables with metabolic outcome measures in the ECM-Ad model were studied using an identical linear mixed model analysis, adjusting for age and gender of the subjects from which either ECM or adipocytes were derived. Means and standard errors of means (error bars) displayed in figures are estimated adjusting for age and gender.

RESULTS:

Adipocyte metabolism is dysregulated in DM:
Human preadipocytes have been shown to retain depot- and patient-specific characteristics in culture (13-15). We generated adipocytes from preadipocytes isolated from VAT and SAT from obese patients undergoing bariatric surgery stratified by diabetes (DM) status. DM patients were older than NDM patients and included more men (**Table 1**). Light microscopy, Oil Red-O staining, and QRTPCR demonstrate that differentiated adipocytes in 2D-culture accumulate cytoplasmic lipid and upregulate expression of adipogenic genes, with no differences between DM and NDM adipocytes with respect to these measures (**Figure 1**)

Basal and insulin-stimulated glucose uptake was decreased in VAT and SAT adipocytes from DM subjects, differences that remained significant after adjusting for age and gender (**Figure**

2A). Linear regression analysis demonstrated a negative correlation between glucose uptake and HbA1c in VAT and SAT adipocytes, correlations that remained significant or approached significance after adjusting for age and gender (**Figure 2B**). No correlations were observed between age and basal or insulin-stimulated glucose uptake in VAT or SAT adipocytes (**data not shown**).

Isoproterenol-stimulated lipolysis, but not basal lipolysis, was decreased in VAT adipocytes from DM compared to NDM subjects, differences that remained significant after adjusting for age and gender. Age-and gender-adjusted basal and isoproterenol-stimulated lipolysis was decreased in SAT adipocytes from DM compared to NDM subjects (**Figure 3A**). Linear regression demonstrated indirect correlations between HbA1c levels and isoproterenol-stimulated lipolysis in VAT adipocytes, and basal lipolysis in SAT adipocytes (**Figure 3B**). No correlations were observed between HbA1c levels and basal lipolysis in VAT adipocytes or isoproterenol-stimulated lipolysis in SAT adipocytes, or between age and basal or isoproterenol-stimulated lipolysis in VAT or SAT adipocytes (**data not shown**).

Lipogenic capacity was evaluated using ^{3}H-acetate incorporation, which was induced by insulin and reduced by C75, a small molecule inhibitor of fatty acid synthase (**Figure 3C**). Age- and gender-adjusted adipocyte lipogenesis did not differ between DM and NDM subjects in VAT or SAT (**Figure 3D**). Linear regression analysis demonstrated no correlations between HbA1c levels or age and lipogenesis in VAT or SAT adipocytes (**data not shown**).

Together these data demonstrate a DM-specific adipocyte metabolic phenotype characterized by defects in glucose uptake and lipolysis.

ECM regulates adipocyte metabolism:

We next studied ECM regulation of adipocyte metabolism using an *in vitro* 3D-culture model utilizing decellularized human adipose tissue as a substrate for preadipocyte growth and adipocyte differentiation. We focused study on ECM and preadipocytes derived from VAT, given its disproportionate role in metabolic disease. Decellularized ECM retains collagen microarchitecture and supports differentiation of preadipocytes into mature adipocytes (**Figure 4**).

To examine the role of ECM-derived signals in regulating adipocyte phenotype, we compared the effect of ECM from DM and NDM VAT on adipocyte metabolic functions. ECM from DM subjects reconstituted with preadipocytes from DM subjects (DM/DM ECM-AD), when compared to ECM from NDM subjects reconstituted with preadipocytes from NDM subjects (NDM/NDM ECM-AD), recapitulated observations in 2D-culture of decreased basal and insulin-stimulated glucose uptake and decreased isoproterenol-stimulated lipolysis (**Figure 5A,B**). Of note, discordance was observed between 2D- and 3D-ECM culture with respect to basal lipolysis, in that DM/DM ECM-AD demonstrated reduced basal lipolysis compared to NDM/NDM ECM-AD (Figure 3), while in contrast, no difference was observed in basal lipolysis between DM and NDM VAT adipocytes in 2D-culture. Controls of "empty" ECM not seeded with preadipocytes demonstrated negligible glucose uptake, lipolysis, and lipogenesis (**data not shown**).

We next examined the hypothesis that ECM can exert DM-specific effects on adipocyte metabolism, by differentiating preadipocytes from DM and NDM VAT in different ECM environments (i.e. ECM from DM and NDM VAT). Differentiation of preadipocytes from DM subjects in NDM ECM (NDM/DM ECM-AD) fully rescued insulin-stimulated glucose uptake and basal lipolysis to levels similar to those observed in NDM/NDM ECM-AD. The glucose uptake rescue effect was attenuated and approached significance after adjusting for age and

gender of subjects from whom both ECM and preadipocytes were derived, while rescue of basal lipolysis remained significant with age-and gender-adjustment of data. Furthermore, age- and gender-adjustment revealed a partial rescue effect of isoproterenol-stimulated lipolysis by NDM ECM on DM preadipocytes (NDM/DM ECM-AD) that was not statistically significant in unadjusted analysis (**Figure 5A,B**).

Conversely, DM ECM inhibited insulin-stimulated glucose uptake in NDM adipocytes, evidenced by experiments in which preadipocytes from NDM subjects were differentiated in DM ECM (DM/NDM ECM-AD), in which insulin-stimulated glucose uptake was suppressed to levels similar to those observed in DM/DM ECM-AD; this effect remained significant with age- and gender-adjustment. In contrast, differentiation of preadipocytes from NDM subjects in DM ECM (DM/NDM ECM-AD) did not decrease basal or isoproterenol-stimulated lipolysis. Finally, basal glucose uptake and lipogenesis were not different between DM/DM and NDM/NDM ECM-AD, and these functions were not regulated by any combination of ECM and adipocytes (**Figure 5A,B**). Taken together, these results demonstrate that the ECM regulates adipocyte metabolism in a disease-specific manner. NDM ECM rescues glucose uptake and basal lipolysis in DM adipocytes, and DM ECM impairs glucose uptake, but not lipolysis, in NDM adipocytes.

To further define the relationship of ECM-adipocyte interactions with DM status, we studied correlations of HbA1c as a continuous variable, of subjects from which ECM was derived (HbA1c-ECM), or subjects from which adipocytes were derived (HbA1c-AD), with metabolic outcome measures, while controlling for age and gender. Both HbA1c-ECM and HbA1c-AD correlated inversely with insulin-stimulated glucose uptake, while HbA1c-ECM correlated inversely with basal lipolysis, and HbA1c-AD correlated inversely with isoproterenol-stimulated lipolysis (**Figure 5C**). No correlations were observed between HbA1c-ECM or HbA1c-AD and basal glucose uptake or lipogenesis (**data not shown**). These data suggest that the diabetic status of the patients from which ECM was derived predominantly dictate basal lipolysis, the diabetic status of the patients from which adipocytes were derived predominantly dictate isoproterenol-stimulated lipolysis, and the diabetic status of both ECM and adipocytes regulate glucose uptake.

To determine if ECM influences adipocyte differentiation, transcript levels of adipogenic genes (ATGL, ACLY, FASN, PPAR-γ) were studied in differentiated ECM-AD tissues. No significant differences in any transcript levels were observed between DM/DM, NDM/NDM, NDM/DM, and DM/NDM ECM-AD groups (**data not shown**), suggesting that differences in differentiation are not a dominant mechanism underlying ECM-adipocyte interactions in the 3D ECM-AD model.

DISCUSSION:

Adipocyte metabolic phenotype in DM:

The specific aberrations in adipocyte metabolism associated with human metabolic disease are poorly defined. We characterize the adipocyte metabolic phenotype associated with DM in obese humans. We confirm impaired glucose uptake as a feature of this phenotype, consistent with prior studies (16-18). The relationship between adipocyte lipogenic phenotype and systemic metabolic disease is controversial. Prior data demonstrate decreased adipose tissue lipogenic gene expression in patients with metabolic disease (19-21), although at least one study demonstrates the opposite (22). Many published reports study gene expression rather than functional assays. Using labeled acetate incorporation into fatty acids, we demonstrate no DM-specific differences in adipocyte lipogenesis in 2D- or 3D-ECM culture, suggesting that alterations in *de novo* lipogenesis do not significantly contribute to adipocyte metabolic

dysfunction in DM. These results do not address other modes of lipid storage in adipocytes, such as triacylglycerol synthesis, issues for future research.

It is relatively well-established that adipose tissue basal lipolysis is increased while beta adrenergic-stimulated lipolysis is decreased in human obesity (23-25). The adipose tissue lipolytic phenotype specific to metabolic disease is less well-defined, with some studies demonstrating increased adipocyte lipolysis in metabolic disease (26, 27), while others demonstrate the opposite (28-31). We demonstrate decreased basal lipolysis in SAT adipocytes and decreased beta adrenergic-stimulated lipolysis in VAT and SAT adipocytes in DM subjects, suggesting that a lipolytic defect characterizes adipocytes in DM. Transgenic manipulations in mice that increase adipocyte lipolysis are associated with favorable metabolic phenotypes (32-34), while gene expression data suggest that decreased lipid processing capacity characterizes insulin-resistant adipose tissue (35, 36). Taken together these observations, along with the established relationship between adipocyte hypertrophy and metabolic disease (4, 37, 38), support our data and suggest that DM is associated with a shift in adipocytes towards a phenotype predisposed to lipid storage (hypertrophy) rather than lipid catabolism (lipolysis).

ECM regulation of adipocyte metabolism:

We and others have demonstrated aberrancies in adipose tissue fibrosis in obesity (1-6), prompting us to explore the role of the ECM in regulating adipocyte metabolism using an *in vitro* model of decellularized human adipose tissue ECM repopulated with preadipocytes that are differentiated into adipocytes within the ECM. Precedent for this model exists, as decellularized tissue models demonstrate independent effects of pulmonary ECM on myofibroblast function (8).

Combining ECM and adipocytes from NDM or DM subjects (i.e. NDM/NDM or DM/DM ECM-AD combinations) recapitulates the metabolic phenotype of isolated adipocytes in standard 2D-culture, but with important differences. For example, we observed concordance between 2D-culture and 3D-ECM culture with respect to DM-specific differences in glucose uptake and beta adrenergic-stimulated lipolysis, but discordance with respect to basal lipolysis, which was similar between DM and NDM adipocytes in 2D-culture, but decreased in DM/DM ECM-AD compared to NDM/NDM ECM-AD in ECM culture. These data suggest that the ECM disproportionately contributes to DM-specific decreases in basal lipolysis, differences that are notably absent in adipocytes in 2D-culture in the absence of ECM. In contrast, basal (non-insulin stimulated) glucose uptake was decreased in DM adipocytes in 2D culture, but similar between DM/DM ECM-AD and NDM/NDM ECM-AD in ECM culture, suggesting that the ECM attenuates defects in basal glucose uptake in the context of DM. Correlations of HbA1c of subjects from which ECM or adipocytes were derived with glucose uptake and lipolysis reinforce these findings, revealing that diabetic status of both ECM and adipocytes each independently contribute to different features of ultimate adipose tissue metabolic phenotype. These observations demonstrate the utility of this model in dissecting distinct effects of ECM on adipocyte metabolism, and speak to distinct roles for ECM and adipocytes in regulating different diabetes-specific features of cellular metabolism.

Most importantly, we demonstrate disease-specific effects of the ECM on adipocyte metabolism: NDM ECM restored insulin-stimulated glucose uptake in DM adipocytes, while conversely, DM ECM reduced insulin-stimulated glucose uptake in NDM adipocytes. Similarly, NDM ECM fully restored basal lipolysis and partially restored beta-adrenergic stimulated lipolysis in DM adipocytes, but conversely, DM ECM had no effect on lipolysis in NDM adipocytes. Finally, no differences in basal glucose uptake or lipogenesis were observed between

any combination of ECM-adipocytes, suggesting that the ECM does not regulate these functions in this model system. Taken together these results demonstrate that NDM ECM has the capacity to restore some but not all features of normal cellular metabolism in DM adipocytes, while DM ECM has the capacity to induce some but not all features of dysfunctional cellular metabolism in NDM adipocytes.

DM subjects are older and include more men than NDM subjects in our cohort, requiring post-hoc age- and gender-adjustment of data. Nonetheless, differences in metabolic outcomes between DM and NDM adipocytes in 2D- and 3D-ECM culture remained significant after adjustment, except for insulin-stimulated glucose uptake in 3D-ECM culture, while in contrast, the rescue effect of NDM ECM on lipolysis was strengthened by age and gender adjustment, primarily due to decreases in basal and beta-adrenergic stimulated lipolysis in DM/DM tissues. These observations suggest that age-and gender-related differences in ECM contribute to its effects on adipocyte metabolism independent of DM status. DM subjects had a higher prevalence of other metabolic diseases and medications, factors which may contribute to different patient-specific effects independent of DM. Subject heterogeneity is an inherent weakness of human studies, and larger studies will be necessary to rigorously address these and other potential confounders. Limited access to lean tissues precluded inclusion of a lean control group, preventing study of obesity-specific ECM effects. Nonetheless ECM effects differed based on the presence or absence of metabolic disease, supporting the clinical relevance of these data. The ECM model lacks multiple adipose tissue constituents, but permits isolated study of specific effects of ECM on adipocytes. We focused study on VAT ECM and adipocytes because of the strong association of VAT with metabolic disease, and limitations in quantities of SAT available. Future research will incorporate other cell types (e.g. macrophages, leukocytes, endothelial cells) and adipose tissue depots into the ECM model, which provides a tractable system to study multiple aspects of adipose tissue biology.

The mechanisms underlying ECM-adipocyte interactions remain unknown. ECM may regulate preadipocyte differentiation with effects on ultimate adipocyte metabolic phenotype. Nonetheless, Oil Red-O staining and adipogenic gene expression was similar between DM and NDM adipocytes in standard 2D culture, and no difference in adipogenic gene expression was observed between groups in 3D-ECM culture. These data argue against a significant intrinsic difference in differentiation capacity between DM and NDM adipocytes or regulation of adipocyte differentiation by the ECM; further study of other aspects of differentiation will be necessary to confirm these observations. ECM interactions with inflammatory cells may influence adipocytes; we have demonstrated differences in IL-4 expression, a pro-fibrotic cytokine, between DM and NDM tissues that correlate with differences in ECM composition (4), suggesting a possible mechanism linking inflammation to fibrosis. Finally, DM-specific alterations in the ECM itself, such as increased advanced glycation end-product glycosylation, may regulate adipocyte metabolism. The ECM-adipocyte culture model provides a tool to study these and other putative mechanisms.

Conclusion:

We demonstrate that human DM is associated with an adipocyte metabolic phenotype characterized by decreased glucose uptake and decreased lipolysis, and that the ECM regulates adipocyte metabolism: NDM ECM partially rescues metabolic dysfunction in metabolically unhealthy adipocytes, while conversely, DM ECM impairs certain features of metabolic function in metabolically healthy adipocytes. These observations suggest the ECM as a target for research directed towards manipulating adipocyte metabolism.

Acknowledgements:
We thank the University of Michigan Center for Statistical Consultation & Research for statistical consultation; Eric White, MD, University of Michigan Department of Internal Medicine for advice and discussion; Colleen Buda, PA, Justin Fahey, PA, Danielle Guerin, NP, Kendra Rogers, PA, and Marilyn Woodruff, NP for assistance with study coordination; SEM performed by University of Michigan Microscopy & Image Analysis Laboratory Biomedical Research Core Facility.

Corresponding Author and person to whom reprint requests should be addressed:
Robert W. O'Rourke, M.D., University of Michigan, Department of Surgery, Section of General Surgery, 2210 Taubman Center-5343, 1500 E. Medical Center Drive, Ann Arbor, MI 48109-5343; Phone: (734) 647-9024; Fax: (734) 232-6188; e-mail: rorourke@umich.edu

Funding: NIH grants R01DK097449 (RWO), R01DK090262 (CNL), T32DK101357 (LAM)

Disclosure: The authors have nothing to disclose.

REFERENCES:

1. Dankel SN, Svärd J, Matthä S, Claussnitzer M, Klöting N, Glunk V, Fandalyuk Z, Grytten E, Solsvik MH, Nielsen HJ, Busch C, Hauner H, Blüher M, Skurk T, Sagen JV, Mellgren G. COL6A3 expression in adipocytes associates with insulin resistance and depends on PPARγ and adipocyte size. *Obesity (Silver Spring).* 2014; 22(8):1807-13.
2. Divoux A, Tordjman J, le Lacasa D, Veyrie N, Hugol D, Aissat A, Basdevant A, Guerre-Millo M, Poitou C, Zucker JD, Bedossa P, Clément K. Fibrosis in human adipose tissue: composition, distribution, and link with lipid metabolism and fat mass loss. *Diabetes* 2010; 59L 2817-25.
3. Lackey DE, Burk DH, Ali MR, Mostaedi R, Smith WH, Park J, Scherer PE, Seay SA, McCoin CS, Bonaldo P, Adams SH. Contributions of adipose tissue architectural and tensile properties toward defining healthy and unhealthy obesity. *Am J Physiol Endocrinol Metab.* 2014; 306(3):E233-46.
4. Muir LA, Neeley CK, Meyer KA, Baker NA, Brosius AM, Washabaugh AR, Varban OA, Finks JF, Zamarron BF, Flesher CG, Chang JS, DelProposto JB, Geletka L, Martinez-Santibanez G, Kaciroti N, Lumeng CN, O'Rourke RW. Adipose tissue fibrosis, hypertrophy, and hyperplasia: correlations with diabetes in human obesity. *Obesity (Silver Spring)* 2016, 24(3):597-605.
5. Spencer M, Yao-Borengasser A, Unal R, Rasouli N, Gurley CM, Zhu B, Peterson CA, Kern PA. Adipose tissue macrophages in insulin-resistant subjects are associated with collagen VI and fibrosis and demonstrate alternative activation. *Am J Physiol Endocrinol Metab.* 2010; 299(6):E1016-27.
6. Sun K, Park J, Gupta OT, Holland WL, Auerbach P, Zhang N, Goncalves-Marangoni R, Nicoloro SM, Czech MP, Varga J, Ploug T, An Z, Scherer PE. Endotrophin triggers adipose tissue fibrosis and metabolic dysfunction. *Nat Commun.* 2014; 5:3485.
7. Chamberlain JJ, Rhinehart AS, Shaefer CF Jr, Neuman A. Diagnosis and Management of Diabetes: Synopsis of the 2016 American Diabetes Association Standards of Medical Care in Diabetes. *Ann Intern Med.* 2016 164(8):542-52.
8. Booth AJ, Hadley R, Cornett AM, Dreffs AA, Matthes SA, Tsui JL, Weiss K, Horowitz JC, Fiore VF, Barker TH, Moore BB, Martinez FJ, Niklason LE, White ES. Acellular normal and

fibrotic human lung matrices as a culture system for in vitro investigation. *Am J Respir Crit Care Med* 2012; 186(9):866-76.
9. Han TT, Toutounji S, Amsden BG, Flynn LE. Adipose-derived stromal cells mediate in vivo adipogenesis, angiogenesis and inflammation in decellularized adipose tissue bioscaffolds. *Biomaterials*. 2015; 72:125-37.
10. Porzionato A, Sfriso MM, Macchi V, Rambaldo A, Lago G, Lancerotto L, Vindigni V, De Caro R. Decellularized omentum as novel biologic scaffold for reconstructive surgery and regenerative medicine. *Eur J Histochem* 2013; 57(1):e4.
11. Akie TE, Cooper MP. Determination of fatty acid oxidation and lipogenesis in mouse primary hepatocytes. *J Vis Exp.* 2015; (102): e52982.
12. Perez-Diaz S, Johnson LA, DeKroon RM, Moreno-Navarrete JM, Alzate O, Fernandez-Real JM, Maeda N, Arbones-Mainar JM. Polymerase I and transcript release factor (PTRF) regulates adipocyte differentiation and determines adipose tissue expandability. *FASEB J.* 2014; 28(8):3769-79.
13. Lee MJ, Fried SK. Optimal protocol for the differentiation and metabolic analysis of human adipose stromal cells. *Methods Enzymol* 2014; 538:49-65.
14. O'Rourke RW, Meyer KA, Gaston G, White AE, Lumeng CN, Marks DL; Hexosamine biosynthesis is a possible mechanism underlying hypoxia's effects on lipid metabolism in human adipocytes. *PLOS One.* 2013; 8(8):e71165.
15. Tchkonia T, Giorgadze N, Pirtskhalava T, Thomou T, DePonte M, Koo A, Forse RA, Chinnappan D, Martin-Ruiz C, von Zglinicki T, Kirkland JL. Fat depot-specific characteristics are retained in strains derived from single human preadipocytes. *Diabetes* 2006; 55:2571–2578.
16. Fabbrini E, Magkos F, Mohammed BS, et al. Intrahepatic fat, not visceral fat, is linked with metabolic complications of obesity. *Proc Natl Acad Sci USA*. 2009; 106(36):15430–15435.
17. Herman MA, Peroni OD, Villoria J, Schön MR, Abumrad NA, Blüher M, Klein S, Kahn BB. A novel ChREBP isoform in adipose tissue regulates systemic glucose metabolism. *Nature*. 2012; 484(7394):333-8.
18. Shepherd PR, Kahn BB. Glucose transporters and insulin action--implications for insulin resistance and diabetes mellitus. *N Engl J Med.* 1999; 341(4):248-57.
19. Fabbrini E, Yoshino J, Yoshino M, Magkos F, Tiemann Luecking C, Samovski D, Fraterrigo G, Okunade AL, Patterson BW, Klein S. Metabolically normal obese people are protected from adverse effects following weight gain. *J Clin Invest.* 2015; 125(2):787-95.
20. Poulain-Godefroy O, Lecoeur C, Pattou F, Frühbeck G, Froguel P. Inflammation is associated with a decrease of lipogenic factors in omental fat in women. *Am J Physiol Regul Integr Comp Physiol* 2008; 295(1):R1-7.
21. Roberts R, Hodson L, Dennis AL, Neville MJ, Humphreys SM, Harnden KE, Micklem KJ, Frayn KN. Markers of de novo lipogenesis in adipose tissue: associations with small adipocytes and insulin sensitivity in humans. *Diabetologia* 2009; 52(5):882-90.
22. Berndt J, Kovacs P, Ruschke K, Klöting N, Fasshauer M, Schön MR, Körner A, Stumvoll M, Blüher M. Fatty acid synthase gene expression in human adipose tissue: association with obesity and type 2 diabetes. *Diabetologia.* 2007; 50:1472–1480.
23. Arner P, Langin D. Lipolysis in lipid turnover, cancer cachexia, and obesity-induced insulin resistance. *Trends Endocrinol Metab.* 2014; 25(5):255-62.
24. Bougnères P, Stunff CL, Pecqueur C, Pinglier E, Adnot P, Ricquier D. In vivo resistance of lipolysis to epinephrine. A new feature of childhood onset obesity. *J Clin Invest* 1997; 99:2568–73.

25. Enoksson S, Talbot M, Rife F, Tamborlane WV, Sherwin RS, Caprio S. Impaired in vivo stimulation of lipolysis in adipose tissue by selective beta2-adrenergic agonist in obese adolescent girls. *Diabetes*. 2000; 49(12):2149-53.
26. Acosta JR, Douagi I, Andersson DP, Bäckdahl J, Rydén M, Arner P, Laurencikiene J. Increased fat cell size: a major phenotype of subcutaneous white adipose tissue in non-obese individuals with type 2 diabetes. *Diabetologia*. 2016; 59(3):560-70.
27. Andersson DP, Löfgren P, Thorell A, Arner P, Hoffstedt J. Visceral fat cell lipolysis and cardiovascular risk factors in obesity. *Horm Metab Res.* 2011; 43(11):809-15.
28. Berndt J, Kralisch S, Klöting N, et al. Adipose triglyceride lipase gene expression in human visceral obesity. Exp Clin Endocrinol Diabetes. 2008; 116(4):203-10.
29. Jocken JW, Langin D, Smit E, Saris WH, Valle C, Hul GB, Holm C, Arner P, Blaak EE. Adipose triglyceride lipase and hormone-sensitive lipase protein expression is decreased in the obese insulin-resistant state. *J Clin Endo Metab* 2007; 92:2292-99.
30. McLaughlin T, Craig C, Liu LF, Perelman D, Allister C, Spielman D, Cushman SW. Adipose cell size and regional fat deposition as predictors of metabolic response to overfeeding in insulin-resistant and insulin-sensitive humans. *Diabetes*. 2016 Feb 16. pii: db151213. [Epub ahead of print]
31. Reynisdottir S, Ellerfeldt K, Wahrenberg H, Lithell H, Arner P. Multiple lipolysis defects in the insulin resistance (metabolic) syndrome. *J Clin Invest* 1994; 93(6):2590-9.
32. Ahmadian M, Duncan RE, Varady KA, Frasson D, Hellerstein MK, Birkenfeld AL, Samuel VT, Shulman GI, Wang Y, Kang C, Sul HS. Adipose overexpression of desnutrin promotes fatty acid use and attenuates diet induced obesity. *Diabetes* 2009; 58: 855-866.
33. Jaworski K, Ahmadian M, Duncan RE, Sarkadi-Nagy E, Varady KA, Hellerstein MK, Lee HY, Samuel VT, Shulman GI, Kim KH, de Val S, Kang C, Sul HS. AdPLA ablation increases lipolysis and prevents obesity induced by high-fat feeding or leptin deficiency. *Nat Med* 2009; 15:159-168.
34. Oh W, Abu-Elheiga L, Kordari P, Gu Z, Shaikenov T, Chirala SS, Wakil SJ. Glucose and fat metabolism in adipose tissue of acetyl-CoA carboxylase 2 knockout mice. *Proc Nat Acad Sci, USA*. 2005; 102(5):1384-1389.
35. Clemente-Postigo M, Queipo-Ortuño MI, Fernandez-Garcia D, Gomez-Huelgas R, Tinahones FJ, Cardona F. Adipose tissue gene expression of factors related to lipid processing in obesity. *PLoS One.* 2011; 6(9):e24783.
36. Soronen J, Laurila PP, Naukkarinen J, Surakka I, Ripatti S, Jauhiainen M, Olkkonen VM, Yki-Järvinen H. Adipose tissue gene expression analysis reveals changes in inflammatory, mitochondrial respiratory and lipid metabolic pathways in obese insulin-resistant subjects. *BMC Med Genomics*. 2012; 5:9.
37. Cotillard A, Poitou C, Torcivia A, Bouillot JL, Dietrich A, Klöting N, Grégoire C, Lolmede K, Blüher M, Clément K. Adipocyte size threshold matters: link with risk of type 2 diabetes and improved insulin resistance after gastric bypass. *J Clin Endocrinol Metab*. 2014; 99(8):E1466-70.
38. Veilleux A, Caron-Jobin M, Noël S, Laberge PY, Tchernof A. Visceral adipocyte hypertrophy is associated with dyslipidemia independent of body composition and fat distribution in women. *Diabetes* 2011; 60(5):1504-11.

Figure 1: Adipocyte 2D-culture: A. Human adipocytes in *in vitro* 2D-culture: Representative photomicrographs of *in vitro* differentiated human VAT and SAT adipocytes (20X top, 40X bottom). B. Adipogenic gene expression in human adipocytes: QRTPCR data comparing

adipogenic gene transcript levels in RNA from human adipocytes differentiated for 14 days *in vitro* to undifferentiated preadipocytes (PA) cultured for 72hrs in non-adipogenic media. Ordinate: fold difference in transcript level in mature adipocytes relative to undifferentiated preadipocyte referent=1; *p<0.001, paired t-test; preadipocytes/adipocytes from n=12 subjects. C. Oil Red-O staining in human adipocytes: Left: Oil Red-O staining quantified by spectrophotometry in human adipocytes. No differences were observed between DM and NDM adipocytes, p>0.520 for VAT and SAT; n=10 DM, 12 NDM subjects for VAT, n=9 DM, 9 NDM subjects for SAT. Right: representative photomicrographs of Oil Red-O stained human adipocytes. D. Adipogenic gene expression in human DM and NDM adipocytes: QRTPCR data comparing adipogenic gene transcript levels in RNA from human DM and NDM adipocytes. Ordinate: fold difference in transcript level in DM adipocytes relative to NDM adipocytes as referent=1; p>0.260 for all comparisons except ATGL (p=0.120) in VAT and FASN (p=0.140) in VAT; n=8 DM, 8 NDM subjects for VAT, n=6 DM, 6 NDM subjects for SAT.

Figure 2: Glucose uptake is impaired in DM adipocytes: A. Glucose uptake is impaired in DM adipocytes: Adipocytes differentiated from VAT or SAT preadipocytes from DM or NDM subjects cultured with or without insulin then studied with glucose uptake assay. Ordinate: age- and gender-adjusted glucose uptake measured by ^{3}H-2D-glucose in cell lysates (cpm) normalized to cell lysate protein concentration (mg/ml); *p<0.050 comparing NDM and DM groups, independent t-test, age-adjusted; n=18 DM, 18 NDM subjects for VAT, n=12 DM, 14 NDM subjects for SAT. B. Glucose uptake correlates inversely with HbA1c: Linear regression analysis correlating VAT adipocyte glucose uptake with HbA1c; ordinate: HbA1c (%); abscissa: glucose uptake, cpm normalized to cell lysate protein concentration (mg/ml); p-values shown are univariate/unadjusted (uv) and age-and gender-adjusted (a/g). HbA1c did not correlate with basal or insulin-stimulated glucose uptake in SAT adipocytes; age did not correlate with basal or insulin-stimulated glucose uptake in VAT or SAT adipocytes.

Figure 3: Lipolysis is decreased in DM adipocytes: A. Lipolysis is impaired in DM adipocytes: Adipocytes differentiated from VAT and SAT preadipocytes from DM or NDM subjects cultured for 72hrs +/- isoproterenol (3mM) then studied with glycerol release assay. Ordinate: age-and gender-adjusted glycerol concentration in cell culture supernatant (mg/ml) normalized to protein concentration of cell lysate (mg/ml); *p<0.050 comparing NDM and DM groups, independent t-test, age- and gender-adjusted; n=20 DM, 19 NDM subjects for VAT, n=13 DM, 12 NDM subjects for SAT. B. Lipolysis correlates inversely with HbA1c: Linear regression analysis correlating HbA1c with isoproterenol-stimulated lipolysis in VAT adipocytes (left) and basal lipolysis in SAT adipocytes (right); ordinate: glycerol release (mg/dl) normalized to cell lysate protein concentration (mg/ml); p-values shown are univariate (uv) and age-and gender-adjusted (a/g); HbA1c did not correlate with basal lipolysis in VAT adipocytes or with isoproterenol-stimulated lipolysis in SAT adipocytes (data not shown); age did not correlate with basal or isoproterenol-stimulated lipolysis in VAT or SAT adipocytes (data not shown). C. ^{3}H-acetate incorporation as a measure of lipogenesis: Human VAT adipocytes cultured 72hrs with ^{3}H-acetate and insulin, insulin + C75 (FASN inhibitor), or no insulin, followed by cell lysis, extraction and scintillation counting of lipid phase. Ordinate: lipogenesis measured by ^{3}H-acetate incorporation into lipid fraction of cell lysate (cpm) normalized to cell lysate protein concentration (mg/ml); *p<0.050 comparing insulin arm with insulin + C75 or no insulin arms, paired t-test, age-adjusted; n=24 subjects total (12 DM, 12 NDM subjects). D. Lipogenesis is similar in DM and NDM adipocytes: Adipocytes differentiated from VAT and SAT

preadipocytes from DM or NDM subjects cultured for 72hrs with ^{3}H-acetate and insulin followed by cell lysis, extraction and scintillation counting of lipid phase. Ordinate: cpm in lipid fraction normalized to cell lysate protein concentration (mg/ml); NS designates p>0.100 comparing NDM and DM groups, independent t-test, age-and gender-adjusted; n=12 DM, 11 NDM subjects for VAT, n= 11 DM, 10 NDM subjects for SAT.

Figure 4: 3D-ECM adipocyte culture: A. ECM-AD model: Adipose tissue is decellularized then repopulated with preadipocytes that are subsequently differentiated within the ECM. B. Decellularized adipose tissue ECM maintains collagen 1 microarchitecture and supports adipocyte differentiation: Top: Collagen 1 immunohistochemistry of whole human VAT before and after decellularization demonstrating maintenance of microarchitecture. Middle: 3D confocal photomicrographs of live human adipocytes within ECM; intact decellularized human VAT stained with Oil Red-O before reseeding with preadipocytes, and 4 days, and 14 days after seeding with preadipocytes followed by adipogenic differentiation; blue: DAPI staining of cell nuclei; red: Oil Red-O staining of intracellular lipid. Bottom: Formalin-fixed, paraffin-embedded, 5µM-sectioned, Oil Red-O-stained human VAT prior to decellularization, immediately after decellularization, and after decellularization, preadipocyte-seeding, and 14 days of adipogenic differentiation, demonstrating cytoplasmic lipid accumulation in adipocytes within ECM. C. Adipocytes in ECM upregulate adipogenic gene expression: QRTPCR data comparing adipogenic gene transcript levels in RNA from human adipocytes differentiated in ECM for 14 days to undifferentiated preadipocytes (PA) in ECM cultured for 72hrs in non-adipogenic media. Ordinate: fold difference in transcript level in mature adipocytes relative to undifferentiated preadipocyte referent=1; all fold differences significant (p<0.001, paired t-test); ECM from 10 subjects, preadipocytes /adipocytes from n=11 subjects. D. Adipose tissue ECM repopulated with adipocytes: Scanning electron micrographs of whole VAT, decellularized VAT, and decellularized VAT seeded with preadipocytes followed by 14 days of adipogenic differentiation.

Figure 5: ECM regulates adipocyte metabolism: A, B. 3D-ECM from DM or NDM subjects seeded with preadipocytes from DM or NDM subjects, differentiated into adipocytes, and studied with metabolic phenotyping. Data bars labeled with patient source (NDM, DM) of ECM and adipocytes (ECM/AD); e.g, NDM/NDM denotes both ECM and preadipocytes derived from NDM patients, while NDM/DM denotes ECM from NDM patients combined with preadipocytes from DM patients. Ordinates: glucose uptake(cpm), normalized to ECM/cell lysate protein concentration(mg/ml); lipolysis: culture supernatant glycerol concentration(mg/ml) normalized to ECM/cell lysate DNA concentration(ng/ml); lipogenesis: ^{3}H-acetate incorporation into lipid fraction of ECM/cell lysate(cpm) normalized to ECM/cell lysate protein concentration(mg/ml); *p<0.050, **p<0.100 comparing indicated data-point to corresponding data-point (basal or insulin-stimulated for glucose uptake, basal or isoproterenol-stimulated for lipolysis) in DM/DM arm, using mixed model analysis adjusting for repeated measures; n= 9 NDM, 8 DM subjects for ECM, 10 NDM, 9 DM subjects for preadipocytes for glucose uptake; 6 NDM, 6 DM subjects for ECM, 6 NDM, 6 DM subjects for preadipocytes for lipolysis; 6 NDM, 6 DM subjects for ECM, 6 NDM, 6 DM subjects for preadipocytes for lipogenesis; (**A**) unadjusted data; (**B**) data adjusted age and gender of subjects for both cell and ECM arms. C. Correlations of glucose uptake and lipolysis, with HbA1c of subjects from which ECM was derived (HbA1c-ECM) or HbA1c from which adipocytes were derived (HbA1c-AD), adjusting for age and gender of subjects from

which ECM were derived for HbA1c-ECM analysis, and adjusting for age and gender of subjects from which adipocytes were derived for HbA1c-AD analysis.

TABLE 1: Subject demographics

	DM (n=27)	NDM (n=43)	p-value*
Clinical characteristics			
Gender (% female)	33%	67%	0.007
Age (mean, S.D., years)	53 (11)	44 (10)	<0.001
BMI (mean, S.D., kg/m^2)	45 (5)	44 (7)	0.860
HbA1c (mean, %)	7.1%	5.6%	<0.001
Comorbid diseases (%)			
Sleep apnea	89%	63%	0.026
Hypertension	85%	51%	0.005
Dyslipidemia	74%	44%	0.025
Medications (%)			
ACE inhibitor	26%	16%	0.368
Beta-blocker	30%	5%	0.010
Insulin	37%	0%	<0.001
Metformin	89%	5%	<0.001
Statin	67%	16%	<0.001
Sulfonylurea	33%	0%	<0.001
Thiazolidinedione	7%	0%	0.145

*Independent t-test was used to compare continuous variables between DM and NDM groups; Fisher's exact test was used to compare dichotomous variables between DM and NDM groups; S.D.: standard deviation

Figure 1

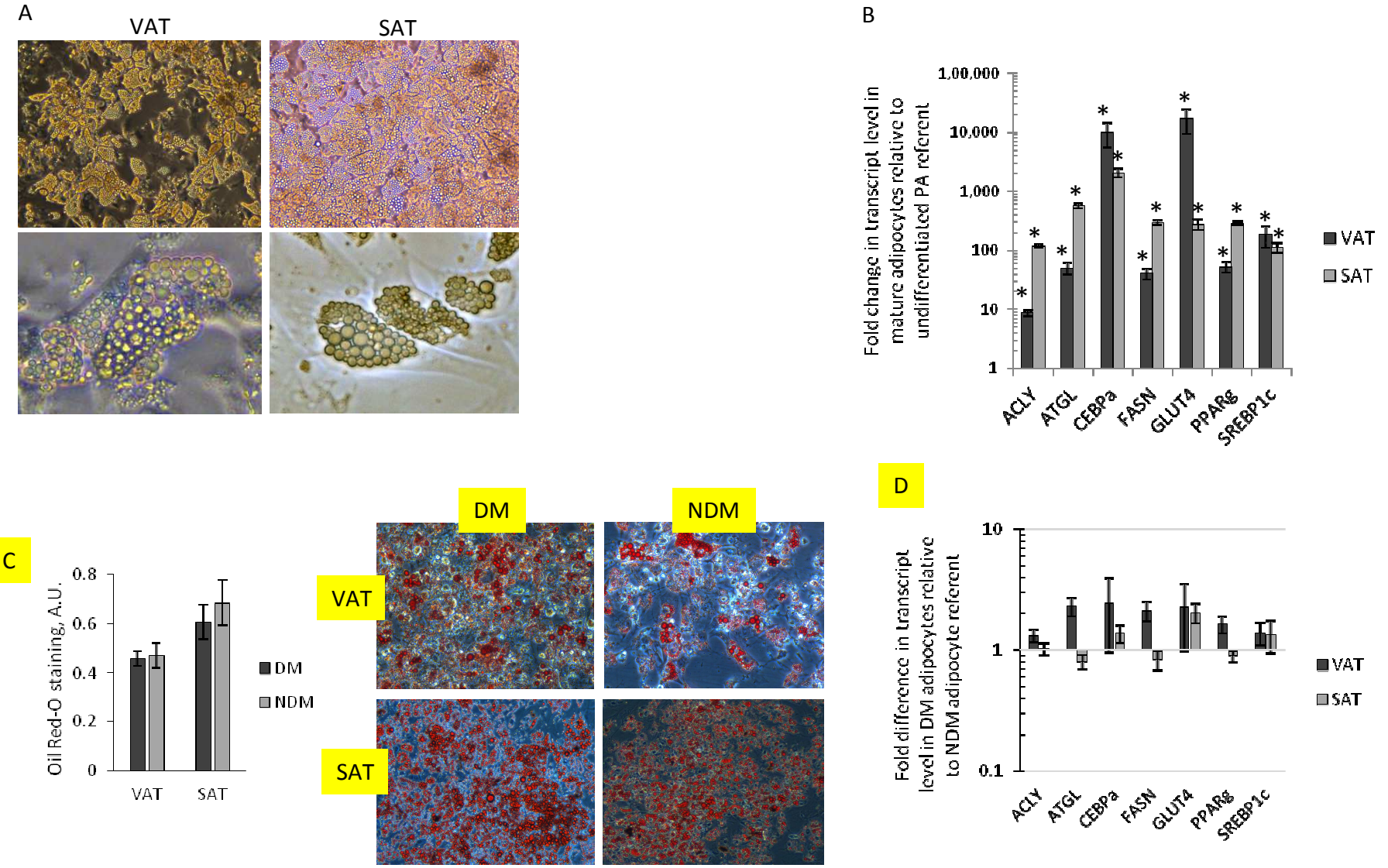

Figure 2

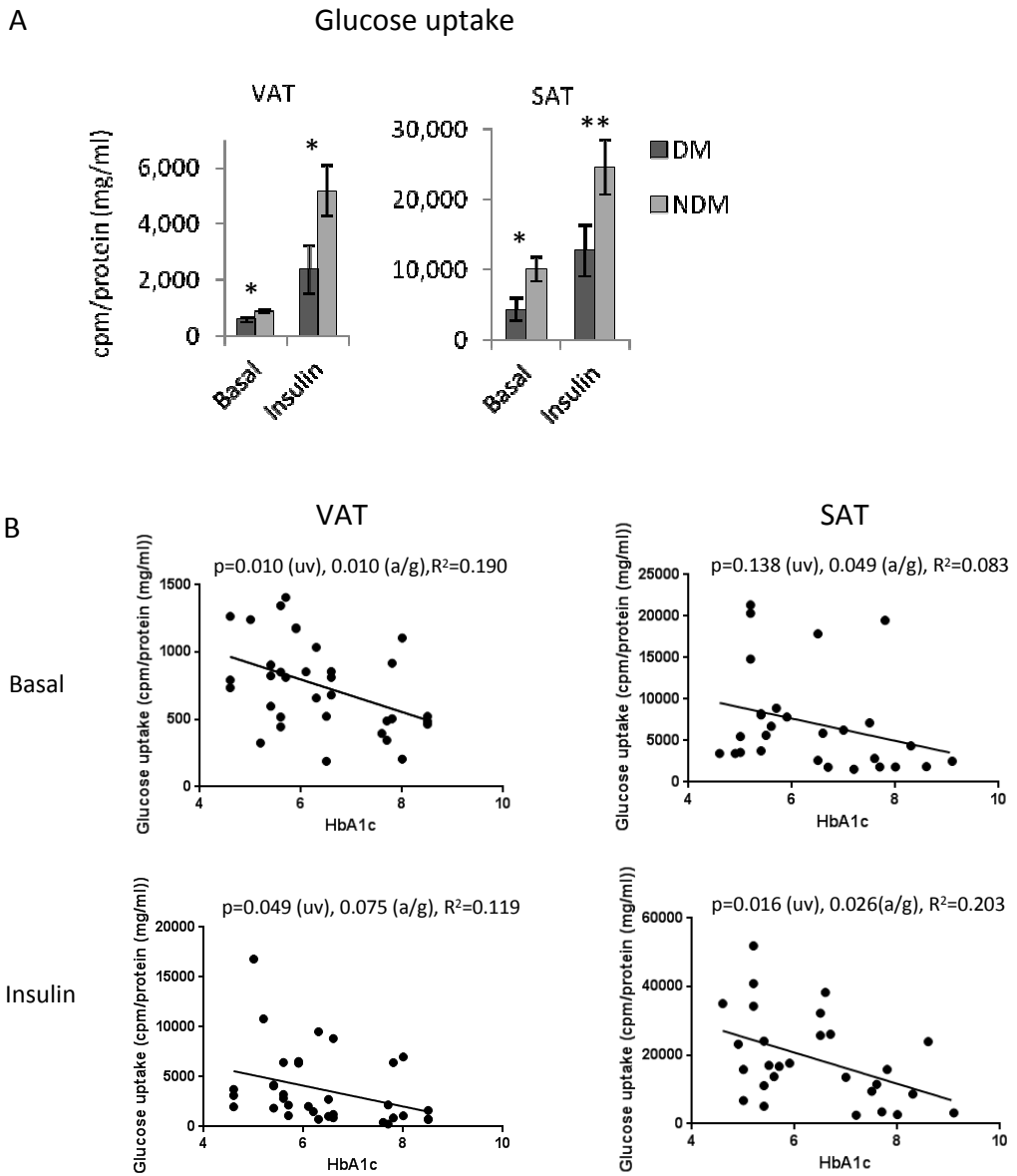

Figure 3

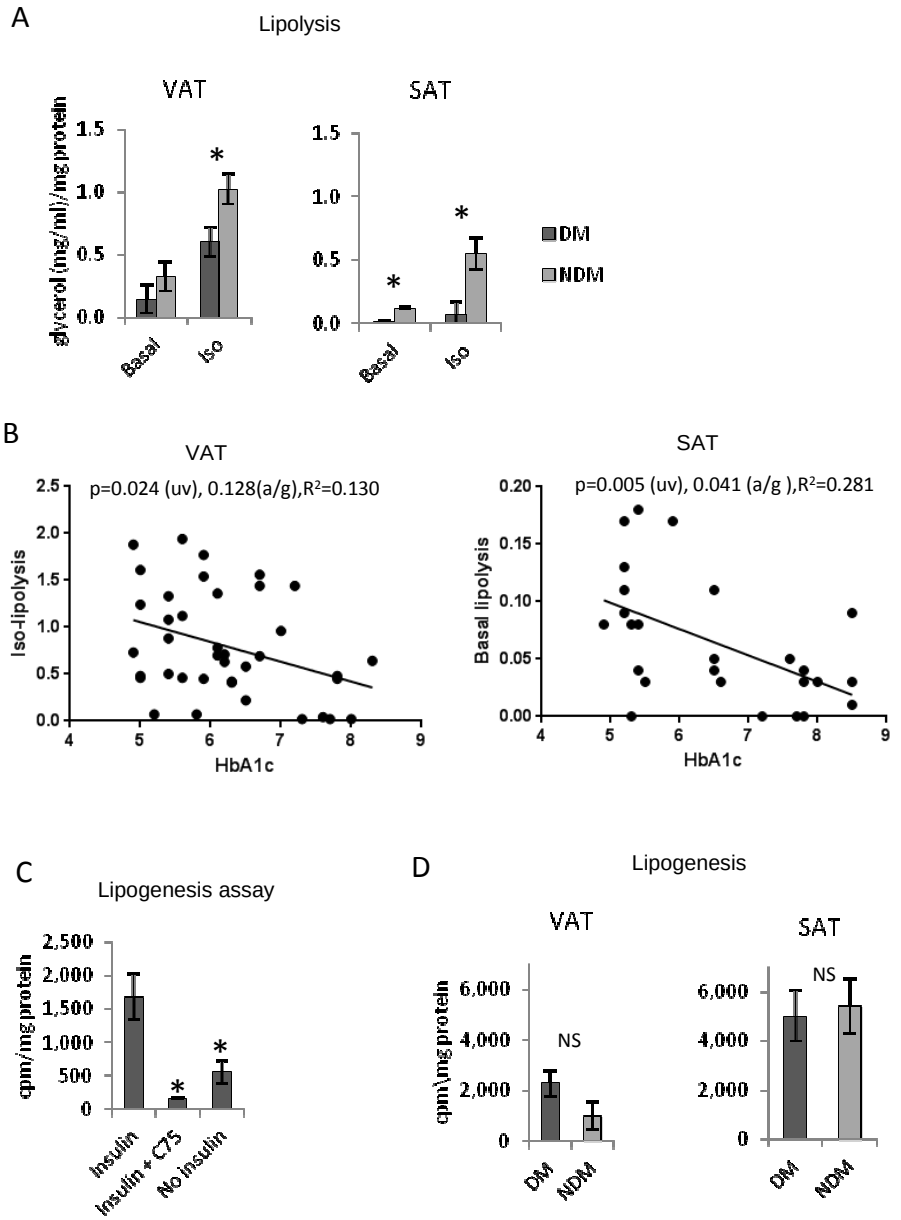

Figure 4

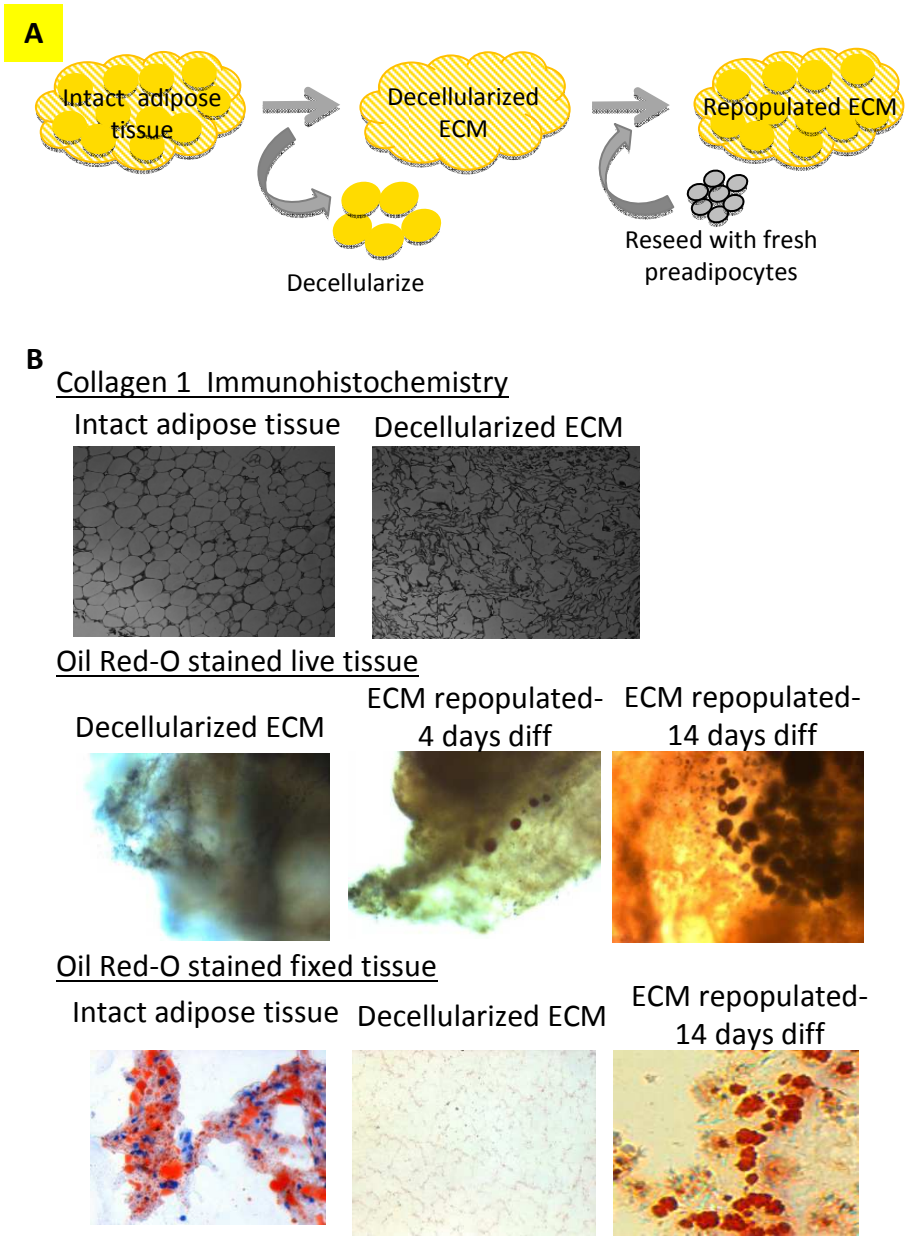

Figure 5

A. Unadjusted

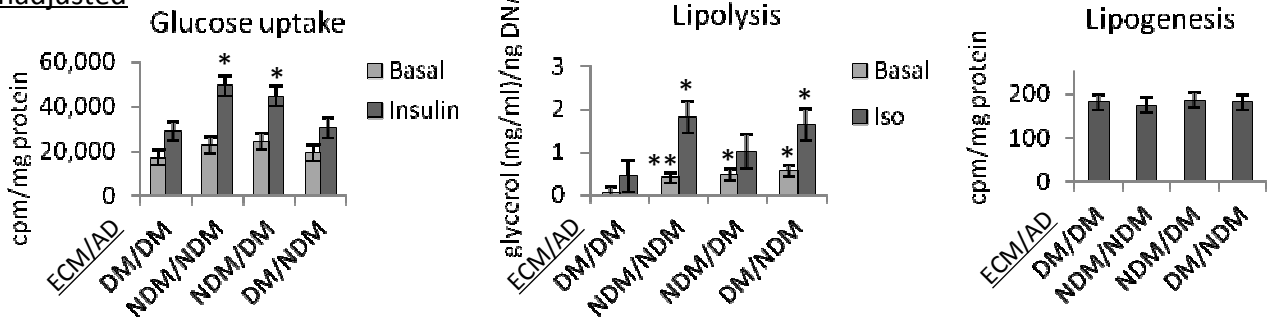

B. Age, gender-adjusted

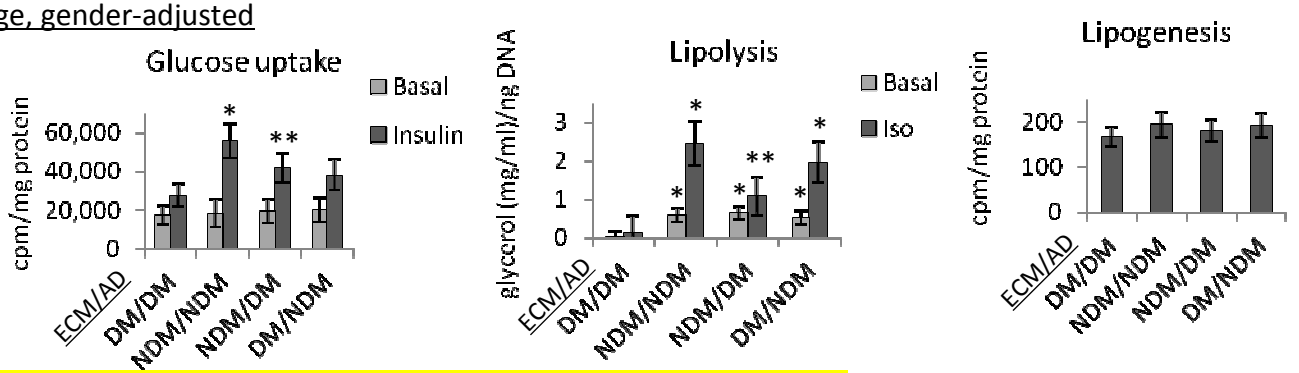

C. HbA1c correlations with glucose uptake, age, gender-adjusted